Nuclear Dynamics in Polyatomic Molecules and High-Order Harmonic Generation

Serguei Patchkovskii*

Steacie Institute for Molecular Sciences, NRC Canada, 100 Sussex Drive, Ottawa, Ontario, K1A 0R6 Canada

(Received 27 February 2009; published 26 June 2009)

High-order harmonic generation in molecular gases is accompanied by short-time evolution of the nuclear vibrational wave function. Using normal coordinate representation, I derive a simple analytical theory of short-time autocorrelation functions and apply it to a test set of 15 small molecules. The results explain large isotope effects observed in CH_4. At the harmonic cutoff in 800 nm driving field, nuclear dynamics reduces the emission intensity from NO and NO_2 molecules by more than 50%. Autocorrelation functions are sensitive to the initial vibrational state, with the nodal structure of the initial vibrational wave packet reflected in the frequency spectrum of the harmonics.

DOI: 10.1103/PhysRevLett.102.253602 PACS numbers: 42.50.Hz, 33.80.Wz

Atomic and molecular gases subjected to intense near-infrared laser fields emit trains of attosecond pulses of high-order harmonic (HHG) radiation. Its spectrum contains information on the electronic and nuclear structure and dynamics [1–3]. Potentially, HHG experiments enable measurements with *simultaneous* attosecond temporal and subangstrom spatial resolution [4–6].

In the standard model [7,8] of high-harmonic generation, an electron is liberated near the peak of the intense laser field. It is then accelerated by the field, and recombines with the parent ion emitting a photon. The intermediate ion exists for a fraction of the laser cycle, with the most energetic photons emitted $\approx 0.65 t_c$ after ionization ($t_c = \frac{2\pi}{\omega}$ is the laser period). At the 800 nm wavelength, cutoff harmonics correspond to the cation existing for only $\approx$1.7 fs—a fleeting time for nuclear dynamics. Only the lightest nuclei are able to move appreciably in this time. The femtosecond-scale nuclear motion has been predicted [9] and observed [10,11] in the lightest molecules—H_2 and D_2, as well as in methane and CD_4. It is widely assumed [2] that molecular HHG could only be affected by the nuclear motion of hydrogen isotopes.

Although the higher mass of other nuclei does decrease the displacements on the HHG time scale, the intensity of harmonic radiation is modulated by the square modulus of the nuclear autocorrelation function [9]:

$$I \propto I_N(t_r) = |\langle \Psi_n(t_r) | \Psi_c(t_r) \rangle|^2 \tag{1}$$

rather than by the displacements *per se*. In Eq. (1), $\Psi_n(t)$ is the vibrational wave packet evolving on the potential energy surface of the neutral species. Wave packet $\Psi_c(t)$ evolves on the cationic surface. Evolution starts at the time of electron's birth ($t = 0$), at which time the two wave packets are assumed to coincide: $\Psi_c(0) = \Psi_n(0)$. The width of the "probe" wave packet Ψ_n scales as $m^{-0.5}$, where m is the effective mass of the oscillator. Because at short times the displacement of Ψ_c decreases as m^{-1}, the two effects partially compensate, and significant modulation of the HHG spectra may occur.

Equation (1) is already an approximation. It assumes that the ionization and recombination amplitudes do not depend on the molecular geometry, no depletion of the ground-state occurs, and that the Born-Oppenheimer potential energy surfaces of both species are not affected by the laser field. Although approximate, Eq. (1) is a useful starting point for studies of polyatomic molecules, where the exact treatment is at present prohibitively expensive.

In the harmonic approximation, vibrational Hamiltonian of the neutral species is given by [12]

$$\hat{H}_n = \sum_i \left\{ -\frac{\hbar^2}{2} \frac{\partial^2}{\partial q_i^2} + \frac{\omega_i^2}{2} q_i^2 \right\}, \tag{2}$$

where the mass-weighted normal coordinates q_i are linear combinations of the Cartesian coordinates r_a:

$$q_i = \sum_a Q_{ai} m_a^{1/2} (r_a - r_a^0), \tag{3}$$

and Q_{ai} and ω_i^2 are, respectively, the eigenvectors and eigenvalues of the mass-weighted Hessian matrix at the equilibrium coordinates $\vec{r}^0$:

$$H_{ab} = m_a^{-1/2} m_b^{-1/2} \frac{\partial^2 U}{\partial r_a \partial r_b}. \tag{4}$$

The eigenfunctions of $\hat{H}_n$ are given by

$$\varphi_\nu(q) = \prod_i \left(\frac{\omega_i}{\pi\hbar} \right)^{1/4} \frac{e^{-z_i^2/2}}{(2^{n_{i\nu}} n_{i\nu}!)^{1/2}} H_{n_{i\nu}}(z_i), \tag{5}$$

where H_k are Hermite polynomials and $z_i = (\omega_i/\hbar)^{1/2} q_i$.

The cationic vibrational Hamiltonian in the region accessed by short-time dynamics is

$$\hat{H}_c = \hat{H}_n + \hat{H}_1 + \tfrac{1}{2}\hat{H}_2, \tag{6}$$

where the gradient ($\hat{H}_1$) and the Hessian ($\hat{H}_2$) coupling terms are evaluated at $\vec{r} = \vec{r}^0$:

$$\hat{H}_1 = \sum_i g_i H_1(z_i), \tag{7}$$

$$\hat{H}_2 = \sum_{i \neq j} h_{ij} H_1(z_i) H_1(z_j) + \sum_i h_{ii} [H_2(z_i) + 2], \tag{8}$$

$$g_i = \frac{1}{2}\sum_a \frac{\partial(U_c - U_n)}{\partial r_a} Q_{ai}\left(\frac{\hbar}{\omega_i m_a}\right)^{1/2}, \quad (9)$$

$$h_{ij} = \frac{1}{4}\sum_{ab} \frac{\partial^2(U_c - U_n)}{\partial r_a \partial r_b} \frac{\hbar Q_{ai} Q_{bj}}{(\omega_i \omega_j m_a m_b)^{1/2}}. \quad (10)$$

The cationic vibrational wave packet is

$$\Psi_c(q,t) = \sum_\nu A_\nu(t)\exp(-\mathrm{i}E_\nu t/\hbar)\varphi_\nu(q), \quad (11)$$

where E_ν is the harmonic vibrational energy of a state ν [$E_\nu = \sum_i (n_{i\nu} + \frac{1}{2})\hbar\omega_i$]. At short times this representation is more compact than the expansion in eigenstates of $\hat{H}_c$, especially for polyatomic molecules. Equation (11) remains applicable when $\hat{H}_c$ is not positive semidefinite.

Substituting Eqs. (7)–(11) into the time-dependent Schrödinger equation for $\hat{H}_c$, I obtain

$$\mathrm{i}\hbar\frac{\partial A_\mu(t)}{\partial t} = \sum_\nu C_{\mu\nu} A_\nu(t)\exp[\mathrm{i}(E_\mu - E_\nu)t/\hbar], \quad (12)$$

$$C_{\mu\nu} = \sum_i (g_i K^{(1)}_{i\mu\nu} + h_{ii} K^{(2)}_{i\mu\nu})\Delta_{i\mu\nu} + \sum_{i<j} h_{ij} K^{(1)}_{i\mu\nu} K^{(1)}_{j\mu\nu}\Delta_{ij\mu\nu}, \quad (13)$$

$$K^{(1)}_{i\mu\nu} = \sqrt{2l_{i\mu\nu}}\,\delta_{|n_{i\mu}-n_{i\nu}|,1}, \quad (14)$$

$$K^{(2)}_{i\mu\nu} = \sqrt{l_{i\mu\nu}(l_{i\mu\nu}-1)}\,\delta_{|n_{i\mu}-n_{i\nu}|,2} + (2n_{i\nu}+1)\delta_{n_{i\mu},n_{i\nu}}, \quad (15)$$

where $\Delta_{i\mu\nu} = \prod_{k\neq i}\delta_{n_{k\mu},n_{k\nu}}$, $\Delta_{ij\mu\nu} = \prod_{k\neq i,j}\delta_{n_{k\mu},n_{k\nu}}$, and $l_{i\mu\nu} = \max(n_{i\mu}, n_{i\nu})$. Expanding $A_\mu(t)$ around $t = 0$ and collecting terms in the same order, I obtain

$$A^{(s+1)}_\mu = -\frac{1}{\hbar}\sum_{r=0}^{s}\sum_\nu C_{\mu\nu} A^{(r)}_\nu \frac{\mathrm{i}^{s-r+1} s!}{r!(s-r)!}\left(\frac{E_\mu - E_\nu}{\hbar}\right)^{s-r}, \quad (16)$$

where $A^{(r)}_\nu$ is the rth derivative of $A_\nu(t)$ at $t = 0$. Finally, for a pure initial vibrational state μ, the nuclear autocorrelation factor [Eq. (1)] becomes

$$I_{N,\mu}(t) = 1 + \sum_{s=1}^{\infty}\frac{1}{(2s)!}B^{(2s)}_\mu t^{2s}, \quad (17)$$

$$B^{(r)}_\mu = \sum_{q=0}^{r}\frac{r!}{q!(r-q)!}(A^{(q)}_\mu)^* A^{(r-q)}_\mu. \quad (18)$$

Equation (17) is subject to all the limitations of Eq. (1). Additionally, it assumes that the initial state is an eigenfunction of harmonic $\hat{H}_n$ and that the wave packets do not leave the region of space where quadratic expansion of the cationic potential energy surface is valid. Its accuracy is expected to improve for shorter times, heavier nuclei, and spatially constrained nuclear motion.

At high expansion orders (s), many of the intermediate amplitudes in Eq. (16) appear repeatedly. Formally, the total number of distinct intermediates grows as $O(s^{d+1})$, where d is the number of vibrational degrees of freedom in the system. The number of numerically significant amplitudes is much smaller. These amplitudes can be stored efficiently as a sparse binary tree [13,14].

Although for practical calculations one would use Eq. (16) directly, qualitative insight is also valuable. For most molecules considered here, the gradient term $\hat{H}_1$ [Eq. (7)] dominates. Neglecting change in the curvature [$\hat{H}_2$, Eq. (8)], the lowest-order term in Eq. (18) for the ground vibrational state is

$$B^{(2)}_0 \approx -\frac{1}{2\hbar}\sum_i \frac{1}{\omega_i}\left(\sum_a \frac{Q_{ai}}{m_a^{1/2}}\frac{\partial U_c}{\partial r_a}\right)^2. \quad (19)$$

Thus, nuclear dynamics is significant whenever the intermediate cationic surface possesses a large gradient along a soft degree of freedom in the neutral species.

Electronic structure calculations on selected molecules use correlation-consistent polarized triple-zeta basis set (cc-pVTZ) [15] and GAMESS-US [16] package. Basis functions with the highest angular momenta (f on C, d on H) are omitted for CH_4. Structures are optimized for the neutral species. Hydrogen molecule calculations use five-orbital complete active space (CAS) wave functions. Diatomic molecules (CO, Cl_2, N_2, F_2, O_2, and NO) use eight-orbital CAS, with the valence ns and np shells included. Triatomic CO_2 and NO_2 use ten-orbital CAS wave functions, while C_2H_4 calculations employ a nine-orbital CAS. Methane's electronic structure is treated with an eight-orbital CAS. In either case, $1s$ core orbitals are not correlated. The heavier C_4H_6 and PF_3 molecules are treated with spin-unrestricted frozen-core second-order Møller-Plesset (MP2) approach. Active spaces and state weights are chosen such as not to lift electronic degeneracies artificially.

Treatment of the electronic structure of methane cation CH_4^+ requires separate discussion. Ionization of the T_d-symmetric CH_4 leads to the intersection point of the three branches of the Jahn-Teller distorted $^2F_2$ state. The initial vibrational wave packet spans all three branches. Its composition depends on the relative orientation of the molecule and the ionizing field, as well as on the subcycle field evolution. A fully satisfactory treatment of the problem requires a coupled simulation of the electronic and nuclear degrees of freedom. For the very short times considered presently, I choose to ignore the nonadiabatic coupling of the electronic surfaces, and treat each branch of the $^2F_2$ surface independently. In order to separate the branches, I apply static electric field of 0.05 atomic units along a C_2 axis of symmetry. The field splits the components of the $^2F_2$ state by $\approx \pm 16$ mH from the barycenter, completely lifting the degeneracy. The results below are for the lowest component of the multiplet. Autocorrelation functions for the remaining two components are numeri-

cally similar. As a consistency test, I also vary splitting fields between 0.04 and 0.08 a.u.

Nuclear factors I_N calculated for the ground-state initial vibrational wave packet are shown in Fig. 1. The fastest dynamics occurs in D_2, H_2, CD_4, and CH_4. Nuclear motion is important for other molecules as well. Thus, for the NO radical nuclear dynamics decreases HHG radiation intensity by a factor of 0.44× at the 800 nm cutoff. A smaller, but still substantial, effect (0.65×) is found for O_2. The modulation is due to the change in equilibrium geometry upon ionization. In both molecules, the chemical bond contracts by $\Delta r \approx -0.17$ bohr upon ionization, producing large forces on the atoms: ≈0.19 a.u. in NO^+, ≈0.13 a.u. in O_2^+. These forces are comparable to the initial gradient in H_2^+ (≈0.14 a.u., $\Delta r \approx +0.59$ bohr).

Less expected is the rapid evolution in NO_2 and PF_3. In the bent NO_2 radical, the ground-state cation is linear. Removal of an electron creates a large force ($g = 6.0 \times 10^{-3}$ hartree) along the 815 cm^{-1} (harmonic) bending mode. The 1470 cm^{-1} symmetric stretch mode is also strongly affected ($g = 6.5 \times 10^{-3}$ H), reflecting the ≈0.10 bohr decrease in the N—O bond length. In PF_3, removal of the lone-pair electron reduces pyramidalization, with the F—P—F angle increasing by ≈10° and the P—F bond shortening by ≈ 0.14 bohr. Large forces arise along the inversion mode ($\nu = 480$ cm^{-1}, $g = 3.2 \times 10^{-3}$ H) and the symmetric stretch mode ($\nu = 900$ cm^{-1}, $g = 5.9 \times 10^{-3}$ H).

One experimental consequence of the short-time nuclear dynamics is the isotope effects in harmonic intensity [9,10]. Deuterium isotope effects as large as 3× were demonstrated in methane. In hydrogen, the calculated ratio of harmonic autocorrelation functions [Fig. 2(a)] shows the same trend, but underestimates the magnitude of the experimental isotope effect. The calculated harmonic ratios are smaller than in the previous anharmonic treatment [9]: 1.16 vs ≈1.3 at 0.8 fs, increasing to 1.35 vs ≈1.5 at 1.7 fs. The discrepancy is likely due to the very large displacements (≈0.5 bohr at 1.7 fs [9]) reached in the H_2^+ cation, which make harmonic approximation inappropriate. Smaller displacements (and therefore better accuracy) are expected for molecules where hydrogen motion is not involved. The remaining deviation from experiment is likely due to the neglect of the electronic contributions, which are particularly important for H_2 [17,18]. In particular, tunneling ionization in H_2 is biased towards longer bond lengths [19], so that the initial wave packet deviates from the pure $\nu = 0$ vibrational ground state of the neutral [20,21]. The difference in recombination dipoles between H_2 and D_2 is also significant for HHG [10].

Despite severe approximations, a reasonable agreement with experiment is found in methane [Fig. 2(b)]. Here, the calculated isotopic ratios are sensitive to the artificial splitting field imposed on the system. The fields I use are comparable to the electric fields present in the experiment (estimated intensity of $\approx 2 \times 10^{14}$ W cm^{-2} [10], $E_{max} \approx$ 0.08 a.u.). As a result, the cationic energy surface is strongly affected by the subcycle evolution of the laser field, making a more rigorous simulation of this system highly desirable.

Remarkably, nuclear autocorrelation function in methane decays *faster* than in lighter hydrogen (Fig. 1), even though a concerted motion is involved in CH_4. The effect arises due to the extreme change in the potential energy surface upon ionization. Both the gradient [Eq. (7) and

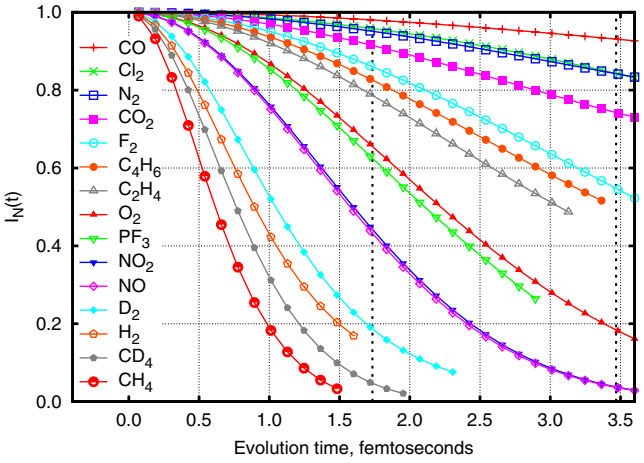

FIG. 1 (color online). Nuclear vibrational factors I_N [Eq. (17)]. Dotted vertical lines correspond to evolution times of the cutoff harmonics for $\lambda = 800$ nm ($t_{cut} \approx 1.73$ fs) and 1600 nm (3.47 fs). The curves continue to the time t where the order-$(N-2)$ expansion deviates from the order-N result. N is 80 for H_2, D_2, NO, CH_4, and CD_4; 32 for CO, F_2, N_2, O_2, and NO_2; 16 for Cl_2 and CO_2; 12 for C_2H_4 and C_4H_6; 10 for PF_3.

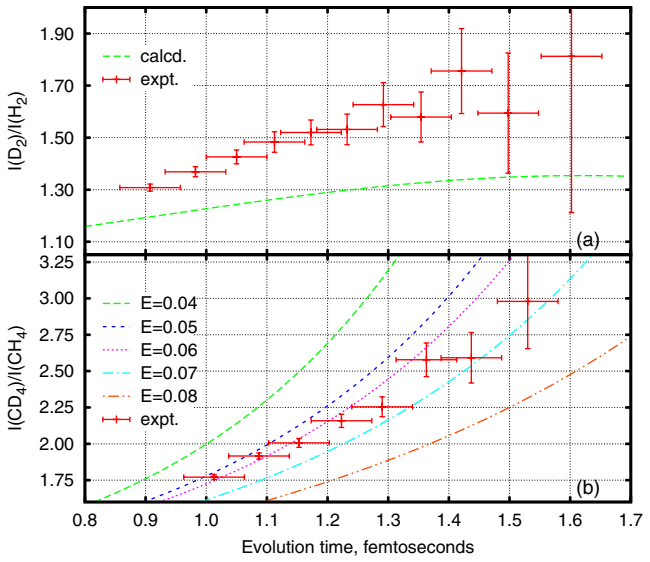

FIG. 2 (color online). Autocorrelation contribution to isotope effects in HHG. Top: D_2 vs H_2. Bottom: CD_4 vs CH_4. For methane, magnitudes of the splitting field (see text) are between 0.04 a.u. (maximum field at laser intensity of $\approx 6 \times 10^{13}$ W cm^{-2}) and 0.08 a.u. ($\approx 2 \times 10^{14}$ W cm^{-2}). Experimental values are from Ref. [10].

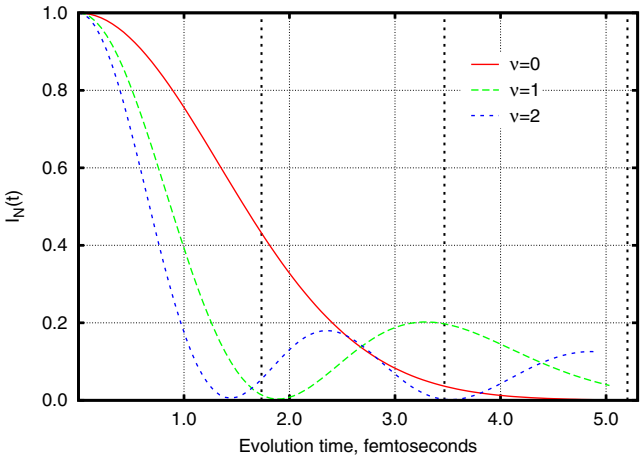

FIG. 3 (color online). Nuclear vibrational factors I_N for pure vibrational states ($\nu = 0$, 1, and 2) of NO radical. Dotted vertical lines are evolution times of the cutoff harmonics at $\lambda = 800$, 1600, and 2400 nm.

curvature [Eq. (8)] terms are large in methane cation, with the change in curvature accounting for about half of the decay rate. Large change in curvature is characteristic of Jahn-Teller cations. Comparable isotope effects may be expected in other spatially degenerate cases.

The final question I would like to address is the dependence of HHG intensities on the nodal structure of the initial vibrational wave function. I consider pure vibrational states of NO. The nuclear factor for the $\nu = 0$ ground vibrational state shows featureless, nearly Gaussian decay pattern (Fig. 3). Excited vibrational states yield faster decay up to ≈ 1.5 fs, as could be expected from the increase in coupling strength with the quantum number ν [Eq. (13)]. However, at slightly longer times, the $\nu = 1$ I_N factor goes to zero at ≈ 1.9 fs, then exhibits a maximum at ≈ 3.1 fs. The $\nu = 2$ autocorrelation function passes through zero at $t \approx 1.4$ and 3.5 fs, and develops local maxima at 2.3 and 4.9 fs, before finally decaying. At a sufficiently long laser wavelength, the nodes of the vibrational wave packet map directly onto the high-harmonic spectrum of vibrationally excited NO. A similar mapping is expected in other systems where the short-time dynamics is dominated by the linear term [$\hat{H}_1$, Eq. (7)] and a single normal mode is excited.

Even in molecules where nuclear autocorrelation factors are not significant for HHG at $\lambda = 800$ nm, they will become more important at longer wavelengths. Indeed, the short-time I_N factors for ground-state initial vibrational wave packets behave as $\approx \exp(-B_0^{(2)} t^2/2)$ with increasing wave packet evolution time.

Nuclear dynamics is a universal and essential feature of high-harmonic generation in molecules, especially at longer wavelengths. It presents both a challenge and an opportunity for the attosecond molecular science. Nuclear dynamics reduces the HHG efficiency in molecules. It may interfere with electronic structure reconstruction techniques [22], otherwise expected to benefit from longer driving field wavelengths. At the same time, nuclear dynamics creates a possibility of a *direct* observation of both amplitudes and phases of vibrational wave packets through the HHG spectra. In principle, the technique could be applicable to small polyatomic molecules as well, provided that ionization does not cause excessive mixing of the normal modes of the neutral species.

I gratefully acknowledge suggestions by P. Corkum, D. Villeneuve, A. Stolow, M. Ivanov, J. P. Marangos, S. Baker, E. Shapiro, and A. Saenz, and partial support by U.S. NSF under Grant No. PHY05-51164.

*Serguei.Patchkovskii@nrc.ca

[1] P. B. Corkum and F. Krausz, Nature Phys. **3**, 381 (2007).
[2] J. P. Marangos, S. Baker, N. Kajumba, J. S. Robinson, J. W. G. Tisch, and R. Torres, Phys. Chem. Chem. Phys. **10**, 35 (2008).
[3] F. Krausz and M. Ivanov, Rev. Mod. Phys. **81**, 163 (2009).
[4] M. Lein, J. Phys. B **40**, R135 (2007).
[5] Y. Mairesse *et al.*, New J. Phys. **10**, 025028 (2008).
[6] S. Gräfe, V. Engel, and M. Y. Ivanov, Phys. Rev. Lett. **101**, 103001 (2008).
[7] P. B. Corkum, Phys. Rev. Lett. **71**, 1994 (1993).
[8] M. Lewenstein, P. Balcou, M. Y. Ivanov, A. L'Huillier, and P. B. Corkum, Phys. Rev. A **49**, 2117 (1994).
[9] M. Lein, Phys. Rev. Lett. **94**, 053004 (2005).
[10] S. Baker, J. S. Robinson, C. A. Haworth, H. Teng, R. A. Smith, C. C. Chirilă, M. Lein, J. W. G. Tisch, and J. P. Marangos, Science **312**, 424 (2006).
[11] T. Kanai, E. J. Takahashi, Y. Nabekawa, and K. Midorikawa, New J. Phys. **10**, 025036 (2008).
[12] E. B. Wilson, Jr., J. C. Decius, and P. C. Cross, *Molecular Vibrations* (Dover, New York, 1980).
[13] D. Gruner and P. Brumer, Chem. Phys. Lett. **138**, 310 (1987).
[14] See EPAPS Document No. E-PRLTAO-103-076928 for the FORTRAN implementation of Eq. (16). For more information on EPAPS, see http://www.aip.org/pubservs/epaps.html.
[15] T. H. Dunning, Jr., J. Chem. Phys. **90**, 1007 (1989).
[16] M. W. Schmidt *et al.*, J. Comput. Chem. **14**, 1347 (1993).
[17] C. C. Chirilă and M. Lein, Phys. Rev. A **77**, 043403 (2008).
[18] A. D. Bandrauk, S. Chelkowski, S. Kawai, and H. Lu, Phys. Rev. Lett. **101**, 153901 (2008).
[19] A. Saenz, Phys. Rev. A **61**, 051402 (2000).
[20] E. Goll, G. Wunner, and A. Saenz, Phys. Rev. Lett. **97**, 103003 (2006).
[21] A. Requate, A. Becker, and F. Faisal, Phys. Rev. A **73**, 033406 (2006).
[22] J. Itatani, J. Levesque, D. Zeidler, H. Niikura, H. Pépin, J. C. Kieffer, P. B. Corkum, and D. M. Villeneuve, Nature (London) **432**, 867 (2004).